ROCKFALL HAZARD AT LITTLE MILL CAMPGROUND, UINTA NATIONAL FOREST: PART 2. DEM ANALYSIS

Thierry Oppikofer[1], Michel Jaboyedoff[2] & Jeffrey A. Coe[3]

[1] *University of Lausanne (e-mail: thierry.oppikofer@unil.ch)*
[2] *University of Lausanne (e-mail: michel.jaboyedoff@unil.ch)*
[3] *U. S. Geological Survey (e-mail: jcoe@usgs.gov)*

Abstract: The scope of this study is the identification of rock slope instabilities and rockfall hazard zones using a digital elevation model. Susceptibility to rockfall initiation is assessed by geometric factors: steepness of topography; possibility of planar or wedge sliding (based on the intersection of four identified discontinuity sets with topography); and erosion potential (erodible volume calculated using a base level method). The runout zones of susceptible rockfall areas are determined using the shadow-angle method.

The study site is a campground in American Fork Canyon (Utah) with a history of rockfall activity. Potential rockfall source areas with low to very high susceptibility are found on both valley flanks (5.85% of the surface of the study area). The campground and a Utah State highway are entirely exposed to rockfall from sources with at least moderate susceptibility. Some parts are exposed to source areas with a high or very high susceptibility.

INTRODUCTION

Morphometric analyses of landslide areas have been made possible by the recent advances in the creation and resolution of digital elevation models (DEMs) (Montgomery *et al.* 1998; Meentemeyer & Moody 2000; Grohmann 2004; Chigira *et al.* 2004; Schultz 2004). DEMs allow for analysis of slope stability (Pack *et al.* 1998; Crosta *et al.* 2001), landslide detection (Baillifard *et al.* 2003; McKean & Roering 2004; Jaboyedoff *et al.* 2004a; Jaboyedoff *et al.* 2004b; Derron *et al.* 2005), and hazard assessments (Baillifard *et al.* 2004).

Quantitative estimates of rock fall hazard combine the probability of failure and the probability of propagation (Leroi, 1996). Propagation of rock fall can be modeled (Agliardi & Crosta 2003) or simply estimated by a geometric rule, like the shadow angle (Evans & Hungr 1993).

Slope instabilities are generally related to several factors. Some of these factors are purely geometric, and may be determined using DEMs. Slope instabilities may develop where:

- topography is steep,
- rock joints or fractures (discontinuities) allow for planar or wedge failure (Hoeck & Bray 1981; Selby 1993),
- rock masses have a high denudation potential (Jaboyedoff *et al.* 2004c).

This study aims to identify large slope instabilities around the Little Mill Campground (Uinta National Forest, Utah, USA) by means of DEM analysis. The developed approach allows the determination of rockfall susceptibility for each DEM cell, and thus the detection of slope instabilities and their propagation zones at various scales.

MORPHOLOGY AND GEOLOGICAL SETTING

Little Mill Campground lies on the bottom of the deeply incised American Fork Canyon and is surrounded by high cliffs of dolomite and limestone. Rockfall activity has been previously documented in the area. Rockfall records are available from about 1990 to 2005. Potential slope instabilities were identified and a preliminary hazard assessment showed that most campsites are downslope from areas with moderate to very high rockfall susceptibility (Coe *et al.* 2005; Coe & Harp 2007). The campground, the geological setting, and the rockfall

problems are described in Part 1 of the overall rockfall study at Little Mill (Coe *et al.* 2007), whereas part 3 (Humble 2007) focuses on the redesign of the campground including rockfall modelling and the implementation of mitigation measures.

DATA

The available digital elevation model (DEM) is part of the National Elevation Dataset (NED) from the U.S. Geological Survey (USGS). The study area is limited to following corner coordinates (N: 40.45769° / E: -111.656681° / S: 40.443365° / W: -111.684286°) and has a cell spacing of about 0.333". For this study, the DEM was transformed into Cartesian XYZ coordinates (based on UTM Zone 12N (NAD 1983), with an individual DEM cell size of 8.85 m. The UTM coordinates of the corners of the study area are: N: 4478791.90 m / E: 444326.23 m / S: 4477172.32 m / W: 441963.24 m).

METHODS

The slope angle of each DEM cell was calculated using standard GIS routines (Burrough & McDonnell 2000). The histogram of the slope angle can be simulated by Gaussian distributions that may be associated with different parts of the topography (Strahler 1950; Rouiller *et al.* 1998). The slope angle above which hillslopes are considered potentially unstable is found where the cliff data distribution becomes dominant over the portions of the histogram represented by other morphometric classes (i.e., valley floor, scree slope, etc.).

In mountainous areas, fractures in the rock mass greatly influence relief and morphology. Assuming that the landscape is shaped by such discontinuities, the analysis of topography permits the determination of the orientation of these discontinuity sets using the software COLTOP 3D. This software computes the slope direction and slope angle of each DEM cell and transforms these into a unique color code for each spatial orientation. By selecting continuous surfaces with the same color, the main slope orientations are obtained. As these orientations are caused by the major discontinuities, the slope direction and slope angle may be correlated to the dip direction and dip angle of the major structural features.

The orientations of these features are used for stability tests, notably, the intersection between these discontinuities with the topography in order to detect zones where planar or wedge failures are possible. For each DEM cell, the software Matterocking 2.0 (Jaboyedoff 2002) calculates the number of discontinuities that may lead to potential planar or wedge sliding according to fracture and slope orientation. A mean fracture spacing of 20 cm is used since field measurements show high variability.

The sloping local base level (SLBL) concept (Jaboyedoff 2004; Jaboyedoff *et al.* 2004c) was applied to determine the erodible masses. It defines a basal surface of erosion above which rocks are considered to be susceptible to erosion by mass wasting within a relatively short period of geologic time (e.g., 20,000 years). An iterative procedure lowers the spurs and spikes of the initial topography to find the SLBL. For the SLBL computation, some points must be fixed; otherwise the final result is flat topography. Assuming that the rivers incise directly into the rock mass, they were considered invariant. Standard GIS routines allow for calculating stream paths using the convergence of DEM cells (Burrough & McDonnell 2000). A fixed point is created once a minimal number of converging pixels (10 pixels in this study) is reached. The SLBL is then calculated between the fixed points. Individual erodible masses are delimited manually by contouring the SLBL surface and by following crests and topographic depressions. Within an individual erodible mass, the volume between the SLBL and the DEM is calculated by multiplying the mass area by the average SLBL residual for the mass, i.e. the relative difference in altitude between the SLBL and the DEM. Jaboyedoff *et al.* (2004c) showed that susceptibility to rockfall initiation increases with the residual, and consequently with the erodible volume.

Combining these factors, the overall rockfall susceptibility can be calculated. Herein, we used a simple multiplication of the three criteria, steepness of the slope, possibility of planar or wedge sliding and high erosion potential. The propagation zones of rockfall originating from these potentially hazardous areas are determined using the shadow-angle method in the software Conefall (Jaboyedoff 2003; Jaboyedoff & Labiouse 2003). The result from applications of the shadow angle method is a map of the area that can be reached by falling rocks from the defined source areas, using a probability of rockfall propagation of 100%). Two variants with different parameters were tested. One uses only the points at the bottom of the cliffs as rockfall source areas, whereas the other uses the entire cliff as potential rockfall sources. A shadow angle of 27.5° from the horizon has been used to determine the propagation zone of blocks starting at the bottom of the cliffs (Evans & Hungr 1993). In the case of the entire cliff as a source area, the shadow angle has been set to 35°. In both cases, a lateral cone aperture of ±20° from the main slope direction was used.

RESULTS

Slope angle

Four Gaussian distributions were identified in the slope angle histogram (Table 1, Figure 1). They can be associated with the bottom of the valley, the scree slopes, the main flanks of the valley, and steep cliffs. For slopes steeper than 51°, the cliff population becomes dominant over the other populations. The cliffs must be considered potential areas for rockfall initiation (Figure 2). These areas are located on both sides of the valley. A large zone in which the topography is steeper than 51° is situated just south of the entrance to the campground. Another large zone lies in the vicinity of the South Fork Ranger Station near the eastern end of the campground.

Table 1. Means and standard deviations of the four Gaussian distributions calculated from the slope angle histogram.

Slope Set Number°	Interpretation	Mean slope (°)	Std. dev. (°)
1	Valley bottom	12.1	6.4
2	Scree slopes	23.4	4.2
3	Valley flanks	38.5	5.9
4	Cliffs	51.0	6.3

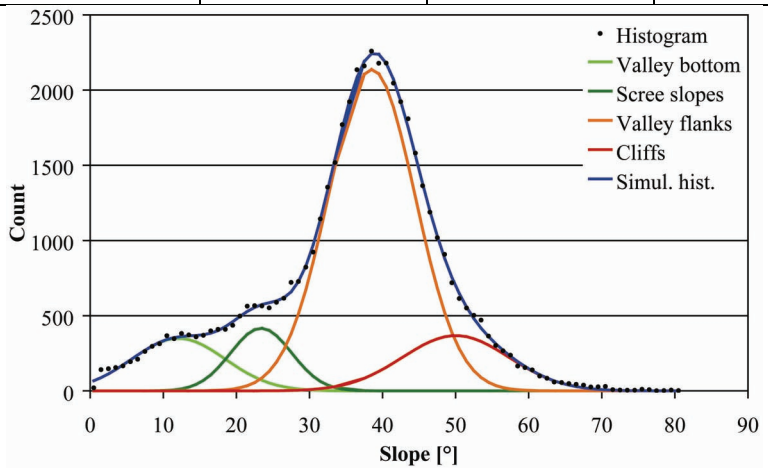

Figure 1. Histogram of the slope angle calculated on the DEM. Four Gaussian populations corresponding to the valley bottom (bright green), the scree slopes (green), the valley flanks (orange) and the cliffs (red) simulate the actual slope histogram. The cliff data set becomes dominant over the other families at a slope angle of 51°.

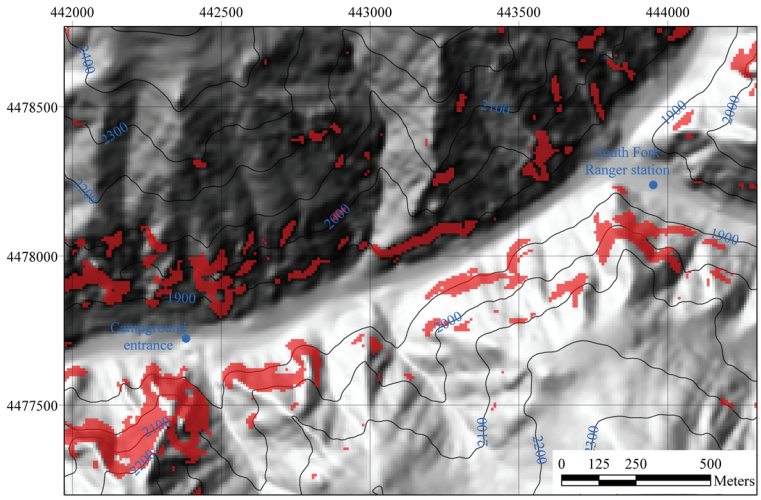

Figure 2. Map of the slopes steeper than 51° (in red) that must be considered as potential areas for rockfall initiation. 100m contour lines, as well as the campground entrance and the South Fork Ranger station are shown for reference.

Structural and morphological analysis

Four major sets of discontinuities (Table 2) can be identified on the DEM. Their orientation cannot be verified since no field measurements are currently (January, 2007) available. The 3D view of the study area (Figure 3) shows the four sets of discontinuities overlain on the topography. Our results from COLTOP 3D also suggest that a NNW-SSE structural lineament (possibly a fault) with an orientation corresponding to discontinuity D3 is present near the center of the study area. The mean dip angles of all four discontinuity sets exceed 40° and thus the common friction angles of discontinuities. Hence they may act as slide planes.

Table 2. Orientation (dip and dip direction) of the discontinuities identified on the DEM using COLTOP 3D.

Set	Color*	Dip direction range [°]	Dip range [°]	Mean
D1	blue	042-081	38-68	060/50
D2	red	156-200	35-70	180/55
D3	yellow	221-259	27-51	240/40
D4	green	281-316	39-66	300/55

* The color corresponds to those used in Figure 3.

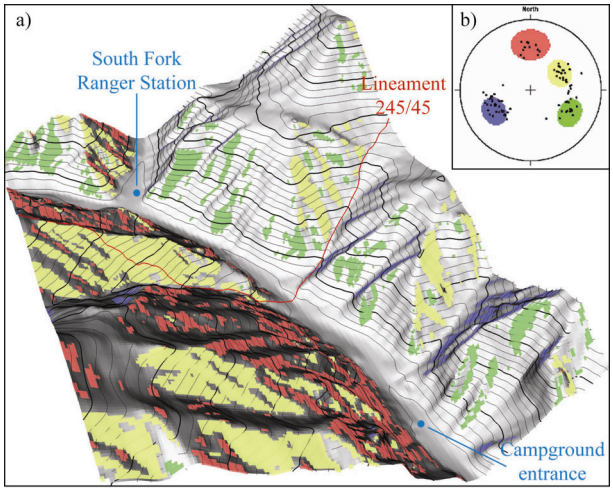

Figure 3. a) Three dimensional view of the Little Mill Campground area from the northwest. Surfaces whose orientations correspond to one of the four discontinuity sets are shown with different colors (see Table 2). The major NNW-SSE lineament is shown in red; b) Stereographic, Lambert, lower hemisphere projection of the poles of some selected DEM cells attributed according to discontinuity set. Colored orientations correspond to mean orientation with a tolerance of ±15° (±20° for D2).

Stability tests

The mean orientations of the four discontinuity sets were intersected with the topography (Figure 5a). The apparent density of intersections at each DEM cell gives a susceptibility for planar or wedge sliding. For joints D1, D2, and D4, up to 50 intersecting discontinuities per cell were computed with a spacing of 1 m. For the joint set D3, the number of discontinuities per cell is 65. Six possible sliding wedge orientations (Figure 4) were intersected with the topography (Figure 5b). The direction of the intersection line, as well as the maximum number of wedge intersections in a DEM cell are given in Table 3. The wedge D1∧D3 (intersection line 150/00) cannot slide.

Table 3. Direction of the wedge axis formed by the intersection of the discontinuity sets and maximum number of intersecting wedges per DEM cell.

Wedge	Intersection	Max. number per cell
D1∧D2	117/33	675
D1∧D3	150/00	0
D1∧D4	003/33	1810
D2∧D3	234/40	400
D2∧D4	240/36	595
D3∧D4	246/40	345

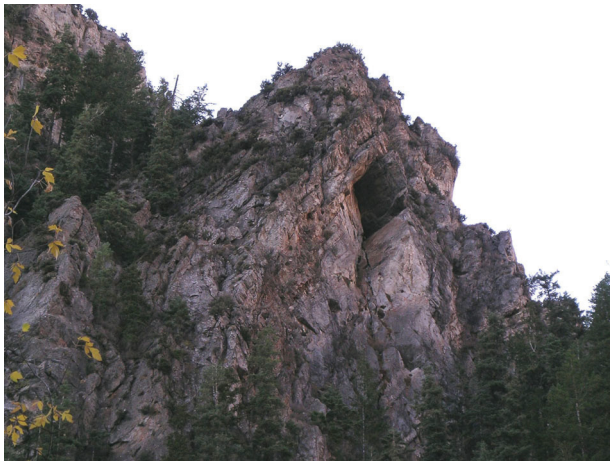

Figure 4. Picture of a sliding wedge on the southern valley side near the west entrance to the campground.

In order to provide a susceptibility level for each of the two sliding mechanisms in a DEM cell, the number of planar discontinuities, as well as the number of sliding wedges were summed and normalized to a number between 0 and 1 by dividing the cell value by the maximal value (Figure 5). The area where wedge sliding is possible is more extensive than the area for planar sliding. This is due to the lower dip angle of the wedge intersection line compared to the dip angle of the discontinuity planes. As with the slope angle criterion, large numbers of sliding planes or wedges are localized on both flanks of the valley. Highest values are found on both sides of the campground entrance, as well as on the cliff south of the South Fork Ranger station.

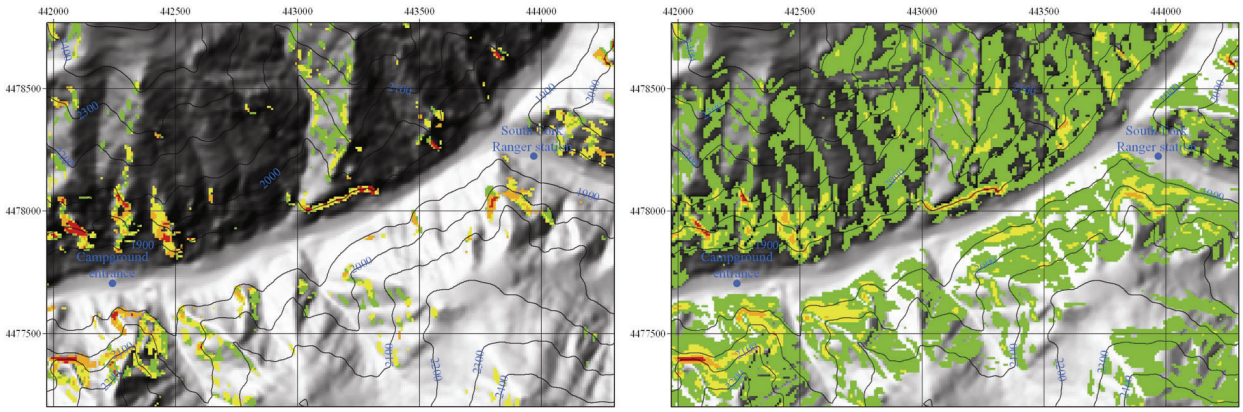

Figure 5. Map of the normalized number of intersections. On the left: a) Discontinuities leading to planar sliding; on the right: b) wedges leading to wedge failures. Legend: green = 0 to 0.1, yellow = 0.1 to 0.25, orange = 0.25 to 0.5, red = 0.5 to 1.0.

Determination of erodible masses

The map of SLBL residuals (contour lines in Figure 6) shows several zones that have a high erosion potential and are susceptible to slope instability. Note that not all the defined volumes are landslides; they are only the volumes that can be eroded. Only a few of them are potential large rockfalls. Maximum residuals (up to 144 m) are found on the south side of the valley side close to the campground entrance. Two hundred and one individual erodible masses were delimited using the contour lines of the SLBL residuals (Figure 6). Their volumes range from 157 m^3 up to 1.71 million m^3. Large volumes, i.e. bigger than 100,000 m^3, are identified on all the valley flanks.

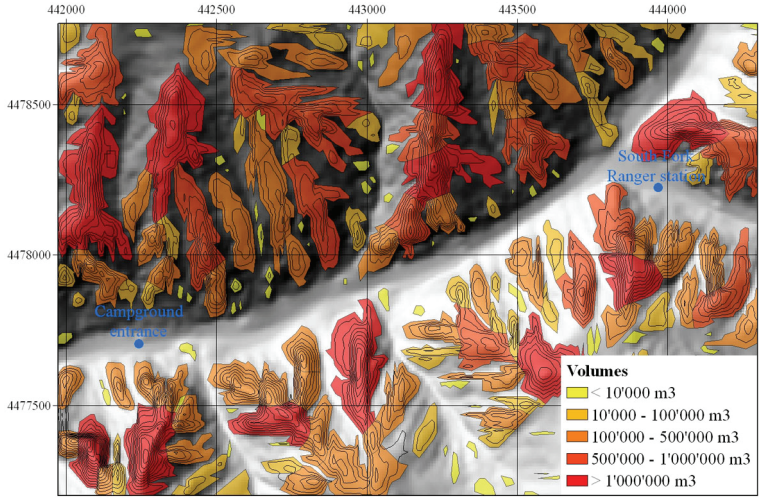

Figure 6. Map of the erodible masses in the area of the Little Mill campground. The black contour lines of the SLBL residuals allowed for delimitation of individual erodible masses (colored polygons). The colors represent the volume contained between the SLBL and DEM surfaces in the respective area.

Synthesis of instability criteria

In order to obtain the susceptibility for rockfall initiation, the three instability criteria needed to be combined. Therefore each criterion was transformed into a classifier ranging from 0 to 1:

- The steep slope criterion was satisfied for cells with slope angles above or equal to 51°.
- The normalized numbers of discontinuities allowing for planar or wedge sliding (corresponding to Figure 5a and 5b) are summed and divided by the maximum value to give a total susceptibility (values between 0 and 1) to failure by a sliding mechanism.
- The erodible volume criterion was weighted by dividing the calculated volumes (Figure 6) by the largest value determined (1.71 million m^3), leading to a graduated value between 0 and 1 for each DEM cell.

The multiplication of these three instability factors leads to an estimation of the rockfall susceptibility. The calculated maximal value of 0.64 is very high. In this DEM cell the slope angle is 80° and the number of planar discontinuities (97), the number of sliding wedges (1705), as well as the volume of the corresponding erodible mass (1.13 millions of m^3) are very high.

Limits have been chosen to delimit zones of very high (>0.25), high (between 0.1 and 0.25), moderate (from 0.01 and 0.1) and low moderate (0.001 to 0.01) rockfall susceptibility (Figure 7). Below a value of 0.001, rockfall hazard is considered low. Approximately 5.85% of the study area is susceptible to rockfall, but only 0.73% of the area shows high or very high rockfall susceptibility (Table 4). These high and very high areas are located on both sides of the valley near the Little Mill Campground entrance, as well as on the cliff south of the South Fork ranger station.

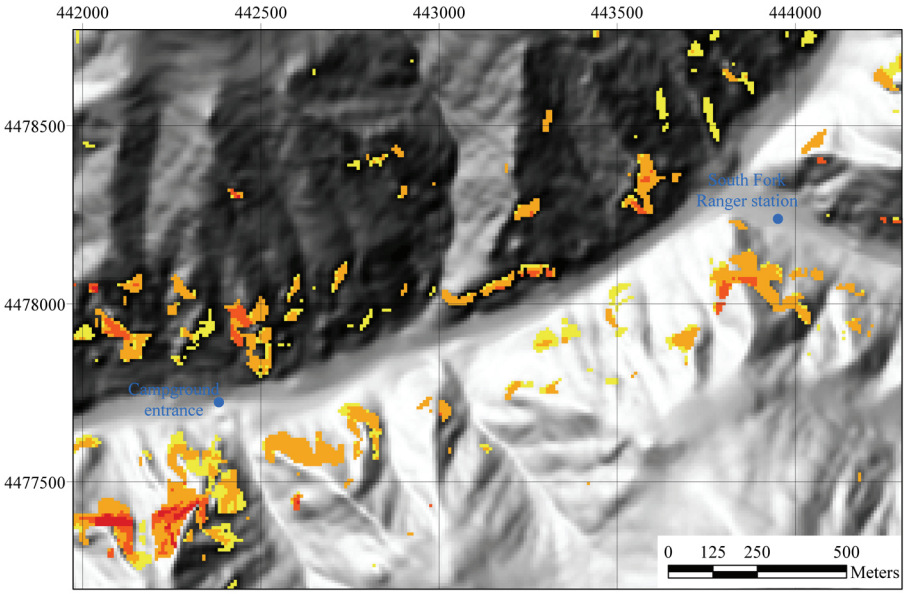

Figure 7. Map of the rockfall susceptibility determined by the combination of the three criteria for slope instability. Legend of the rockfall susceptibility: low = no color; yellow = low moderate; orange = moderate; orange-red = high; red = very high.

Table 4. Cell count and percentage of the calculated rockfall susceptibility

Rockfall susceptibility	Cells	Percentage	
Low (<0.001)	46001	94.15%	
Low Moderate (0.001 - 0.01)	820	1.68%	5.85%
Moderate (0.01 - 0.10)	1682	3.44%	
High (0.10 - 0.25)	287	0.59%	
Very high (>0.25)	71	0.15%	
Sum	48861	100.00%	

Rockfall propagation

For the different degrees of rockfall susceptibility, the corresponding runout distances were mapped using the shadow-angle method. For both variants (27.5° shadow angle starting at the bottom of the cliffs and 35° shadow angle using all the rockfall source cells) the propagation areas of rockfall initiating in cells with moderate, high or very high susceptibility are shown in Figure 8.

A shadow-angle of 27.5° gives a larger runout zone than a 35° shadow angle. In both cases, Little Mill campground and about 700 meters of Highway 92 may be reached by rockfall initiating in zones of very high susceptibility. The western and eastern parts of the campground, South Fork Ranger station, and more than 1.7 km of the highway (2000 meters for a shadow-angle of 27.5°, 1750 meters for the 35° angle) are exposed to rockfall from high susceptibility areas. Considering the runout zones of moderate susceptible rockfall sources, the entire bottom of the canyon is potentially exposed.

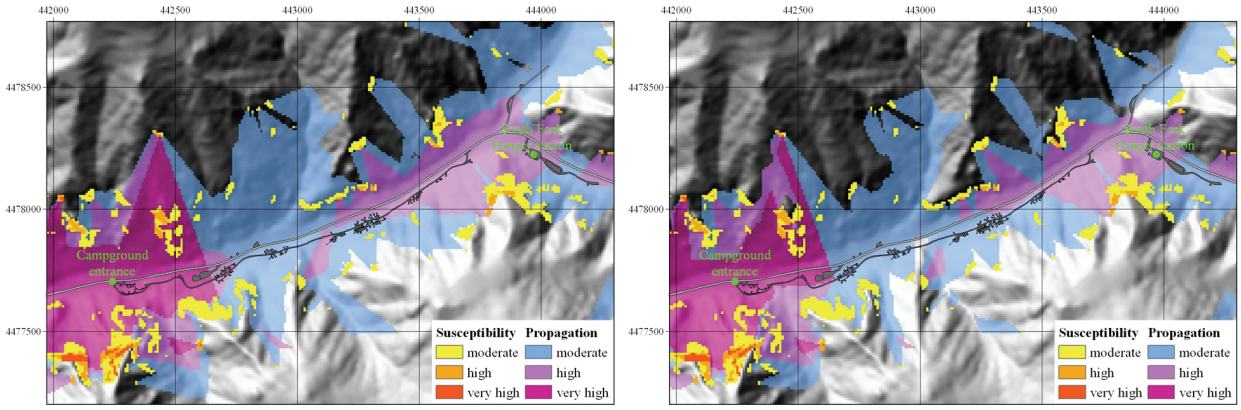

Figure 8. Propagation zones of rockfall initiating in DEM cells with moderate, high, or very high rockfall susceptibility using the shadow angle method. Left) a shadow angle of 27.5° with rocks falling from the bottom of the cliffs; Right) a shadow angle of 35° with rocks falling from the entire cliff area. Highway 92 (grey) and the campsites (dark grey) of the Little Mill Campground (taken from Coe *et al.* 2005) are objects at risk.

CONCLUSIONS

The rockfall propagation zones derived from high and very high susceptible sources affect the areas near the entrance and exit of the Little Mill Campground, as well as the South Fork Ranger station. When the propagation zones from areas with moderate rockfall susceptibility are considered, the entire floor of the canyon is exposed to rock fall hazards. The analysis of digital elevation models permits a precise delineation of potential rockfall hazard zones.

The comparison between the rockfall initiation zones of the USGS preliminary rockfall hazard map (Coe *et al.* 2005, Coe & Harp 2007) and the rockfall susceptibility map of this study shows a good correspondence even though two very different assessment methods were used. Zones with high to very high rockfall susceptibility derived from DEM analysis fall generally in the rockfall initiation zones of the preliminary hazard map but provide more details. The DEM analysis provides a more refined map of potential rockfall source areas compared to the USGS map. On the other hand, the hazardous areas calculated from the DEM are more extensive than those shown on the USGS map because the shadow-angle method is conservative (from a hazards perspective) and provide maximum rockfall runout zones.

DEM analyses of rockfall prone areas have become a very useful tool for preliminary hazard assessment. These analyses allow for a rapid estimation of the potential rockfall sources and runout zones. They can thus be used to supplement or focus detailed field investigations.

The method presented in this study needs further refinement. Most notably, the determination of rockfall source areas using rockfall susceptibility has to be improved.

Corresponding author: Thierry Oppikofer, University of Lausanne, Institute of Geomatics and Analysis of Risk (IGAR), CH-1015 Lausanne, Switzerland; Tel: +41 21 692 35 42. Email: thierry.oppikofer@unil.ch

REFERENCES

AGLIARDI, F. & CROSTA, G. 2003 High resolution three-dimensional numerical modelling of rockfalls. *International Journal of Rock Mechanics and Mining Sciences*, **40**, 455-471.

BAILLIFARD, F., JABOYEDOFF, M. & SARTORI, M. 2003. Rockfall hazard mapping along a mountainous road in Switzerland using an empirical approach. *Natural Hazards and Earth System Sciences*, **3**, 435-442.

BAILLIFARD, F., JABOYEDOFF, M., ROUILLER, J.-D., COUTURE, R., LOCAT, J., LOCAT, P., ROBICHAUD, G. & HAMEL, G. 2004. Towards a GIS-based hazard assessment along the Quebec City Promontory, Quebec, Canada. *In:* LACERDA, W.A., EHRLICH., M., FONTOURA, A.B. & SAYO, A. (eds.) *Landslides Evaluation and Stabilization*. Balkema, Rotterdam, 207-213.

BURROUGH, P.A. & MCDONNELL, R.A. 2000. *Principals of Geographical Information Systems*. Oxford University Press, Oxford, 333p.

CHIGIRA, M., DUAN, F., YAGI, H. & FURUYA, T. 2004. Using an airborne laser scanner for the identification of shallow landslides and susceptibility assessment in an area of ignimbrite overlain by permeable pyroclastics. *Landslides*, **1** (2004), 203–209.

COE, J.A. & HARP E.L. 2007. Influence of tectonic folding on rockfall susceptibility, American Fork Canyon, Utah, USA. *Natural Hazards and Earth System Sciences*, **7**, 1-14.

COE, J.A., HARP E.L., TARR, A.C. & MICHAEL, J.A. 2005. Rock-Fall Hazard Assessment of Little Mill Campground, American Fork Canyon, Uinta National Forest, Utah. U.S. Geological Survey Open-File Report 2005–1229, Reston (Virginia), 50p.

COE, J.A., HARP E.L., TARR, A.C. & MICHAEL, J.A. 2007. Rockfall hazard at Little Mill Campground, Uinta National Forest: Part 1. Geologic hazard assessment. This volume, 15p.

CROSTA, G., FRATTINI, P. & STERLACCHINI, S. 2001. Valutazione e gestione del rischio da frana. Regione Lombardia, Milano, 169.

DERRON, M.-H., BLIKRA, L. & JABOYEDOFF, M. 2005. Preliminary Assessment of Landslide and Rockfall Hazards using a DEM (Oppstadhornet, Norway). *Natural Hazards and Earth System Sciences*, **5**, 285-292.

EVANS, S. & HUNGR, O. 1993. The assessment of rockfall hazard at the base of talus slopes. *Canadian Geotechnical Journal*, **30**, 620-636.

GROHMANN, C.H. 2004. Morphometric analysis in geographic information systems: applications of free software GRASS and R. *Computers and Geosciences*, **30**, 1055-1067.

HOEK, E. & BRAY, J. 1981. *Rock slope engineering, revised third edition*. E&FN Spon, London, 358p.

HUMBLE, J.P.E. 2007. Rockfall hazard at Little Mill Campground, Uinta National Forest: Part 3. Rockfall modeling and campground redesign. This volume, 9p.

JABOYEDOFF, M. 2002. Matterocking 2.0: A program for detecting rockslide instabilities. Crealp, Sion, http://www.crealp.ch.

JABOYEDOFF, M. 2003. Conefall 1.0: A program to estimate propagation zones of rockfall, based on cone method. Quanterra, Lausanne, http://www.quanterra.ch.

JABOYEDOFF, M. 2004: Sloping Local Base Level an insight to the definition of the volume implied in gravitational earth crust movements. *32nd International Geological Congress (32IGC) August 20-28 2004, Firenze, Italy*.

JABOYEDOFF, M., BAILLIFARD, F., PHILIPPOSSIAN, F. & ROUILLER, J.-D. 2004a. Assessing the fracture occurrence using the "Weighted fracturing density": a step towards estimating rock instability hazard. *Natural Hazards and Earth System Sciences*, **4**, 83-93.

JABOYEDOFF, M., BAILLIFARD, F., COUTURE, R., LOCAT, J. & LOCAT, P. 2004b. New insight of geomorphology and landslide prone area detection using DEM. *In:* LACERDA, W.A., EHRLICH, M., FONTOURA, A.B. & SAYO, A. (eds.) *Landslides Evaluation and stabilization.* Balkema, Rotterdam, 199-205.

JABOYEDOFF, M., BAILLIFARD, F., COUTURE, R., LOCAT, J. & LOCAT, P. 2004c. Toward preliminary hazard assessment using DEM topographic analysis and simple mechanic modelling by means of sloping local base level. *In:* LACERDA, W.A., EHRLICH, M., FONTOURA, A.B. & SAYO, A. (eds.) *Landslides Evaluation and stabilization.* Balkema, Rotterdam, 191-197.

JABOYEDOFF, M. & LABIOUSE, V. 2003. Preliminary assessment of rockfall hazard based on GIS data. *ISRM 2003 - Technology roadmap for rock mechanics, Symposium Series*. South African Institute of Mining and Metallurgy, **1**, 575-578.

LEROI, E. 1996. Landslides hazard – risk maps at different scales: objectives, tools and developments. *In Proceedings of the 7th Int. Symp. on Landslides, Trondheim, Norway*, **1**, 35-51.

MCKEAN, J. & ROERING, J. 2004. Objective landslide detection and surface morphology mapping using high-resolution airborne laser altimetry. *Geomorphology*, **57**, 331–351.

MEENTEMEYER, R.K. & MOODY, A. 2000. Automated mapping of conformity between topographic and geological surfaces. *Computers and Geosciences*, **26** (7), 815-829.

MONTGOMERY, D. R., DIETRICH, W. E. & SULLIVAN, K. 1998. The role of GIS in watershed analysis. *In:* LANE, S. N., RICHARDS, K. S. & CHANDLER, J. H. (eds) *Landform monitoring, modelling and analysis*. J. Wiley and Sons, New-York, 241–262.

PACK, R. T., TARBOTON, D. G. & GOODWIN, C. N. 1998. The SINMAP approach to terrain stability mapping. *In: Proceedings 8th Congress of the International Association of Engineering Geology, Vancouver, British Columbia, Canada, 21–25 September 1998,* 1157–1165.

ROUILLER, J.-D., JABOYEDOFF, M., MARRO, C., PHLIPPOSSIAN, F. & MAMIN, M. 1998. *Pentes instables dans le Pennique valaisan - MATTEROCK: une méthodologie d'auscultation des falaises et de detection des éboulements majeurs potentiels. Rapport final PNR 31.* VDF, Zürich, 239p.

SELBY, M.J. 1993. *Hillslope materials and processes, 2nd edition*. Oxford University Press, Oxford, 451p.

STRAHLER, A.N. 1950. Equilibrium theory of erosional slopes approached by frequency distribution analysis. *American Journal of Science,* **248**, 673-696, 800-814.

SCHULZ, W.H. 2004. Landslides mapped using LIDAR imagery. U.S. Geological Survey Open-File Report 2004-1396, Seattle (Washington), 12 p.